Synthesis, Crystal structure, in vitro, and in silico biological studies of 2, 5-dihydroxybenzaldehyde based novel Schiff bases

minakshee todarwal
KKHA Arts, SMGL Commerce, and SPHJ Science College
Rakesh S. Sancheti
KKHA Arts, SMGL Commerce, and SPHJ Science College
Hakikulla H. Shah
KKHA Arts, SMGL Commerce, and SPHJ Science College
Arvind M. Patil
KKHA Arts, SMGL Commerce, and SPHJ Science College
Rahul D. Patil
KBC, North Maharashtra University
Ratnamala S. Bendre (bendrers@rediffmail.com)
KBC, North Maharashtra University

Research Article

Keywords: Schiff base, 2, 5-dihydroxybenzaldehyde, single crystal, Antibacterial, Antifungal, β-ketoacyl-ACP synthase-I

Posted Date: January 25th, 2023

DOI: https://doi.org/10.21203/rs.3.rs-2497292/v1

Abstract

The present study reports the synthesis of novel Schiff base ligands (S_1-S_8) derived from 2, 5-dihydroxybenzaldehyde by coupling with substituted amines. Further, the electron-donating and electron-withdrawing substituents on the amines are intended to tune the properties of the new Schiff base ligands. The chemical structures of these compounds were extensively elucidated by FT-IR, ^{1}H-NMR, ^{13}C-NMR, and ESI-MS. The X-ray analyses show that the compounds crystallized in a triclinic crystal system with a space group of P-1 and Z = 2 for S_1. Besides, antimicrobial potency against gram-positive bacteria and gram-negative bacteria, as well as against fungi, was studied. S_3 has superior inhibitory activity against all bacterial strains. The consortium of different substituent atoms on the phenyl ring and the heterocyclic ring counterpart is one of the reasons behind the recorded optimal activity. Compound S_8 has potent antifungal inhibitory action against *C.albicans* compared to the standard antifungal, whereas Schiff base S_5 also has well to moderate activity against all fungal strains. A molecular docking result indicates that these compounds could also be effective against the resistance β-ketoacyl-ACP (acyl carrier protein) synthase-I enzyme of *E.coli*.

Highlights

1. Design and synthesis of new Schiff bases S_1-S_8 from 2, 5-dihydroxybenzaldehyde.
2. Various Spectroscopic techniques were used to characterize synthesized compounds.
3. The crystal structure has been established by single-crystal X-ray diffraction.
4. In vitro antimicrobial activity, the study showed encouraging results.
5. A molecular docking study shows strong binding interactions with β-ketoacyl-ACP (acyl carrier protein) synthase-I enzyme of *E.coli.*

1. Introduction

The number of people suffering from infectious diseases that require life-long treatment and are brought on by multi-drug resistant Gram-positive and Gram-negative pathogen bacteria has risen alarmingly over the past few decades.[1] It is now the second most significant cause of mortality worldwide. The condensing protein β-ketoacyl-ACP (acyl carrier protein) synthase-I is a crucial target for developing innovative antibacterial drugs among the related FAS II (Fatty Acid Synthase) enzymes.[2, 3]

2,5-dihydroxybenzaldehyde is a naturally occurring antimicrobial compound called gentisaldehyde, which inhibits the growth of *Mycobacterium avium subspecies paratuberculosis.* 2,5-dihydroxybenzaldehyde is active against *S. aureus* strains with an MIC_{50} (500 mg/L).[4–6] Many polyhydroxy phenolic compounds have antimicrobial, anti-carcinogenic, and anti-mutagenic activities useful for several medicinal applications.[7] Several phenolic compounds are potent therapeutic agents for curing stomach and kidney problems and have good anti-inflammatory activity.[8] The Discovery of Schiff bases has drawn

much attention due to easy formation by incorporating substituted aldehydes and amine precursors, which may bring variation in the fundamental properties of the synthesized products.

The ease with which the Schiff bases are designed and synthesized has made them be referred to as fortunate ligands.[9] Schiff bases are a significant class of organic and bioinorganic compounds because they have substantial pharmacological activities such as cytotoxicity, DNA cleavages, antifungal, antibacterial, antimalarial, antiproliferative, anti-inflammatory, antiviral, antioxidant, anticancer, analgesic, antipyretic, antidiabetic and anti-HIV activities.[10–24] Schiff bases containing heterocycles have drawn much attention due to their diverse biological activity.[25] Extra hydroxyl group at ortho and para position with respect to imines linkage increases antifungal activity against *C.albicans* fungi.[7] Schiff bases of chlorine-substituted aniline and salicylaldehyde showed higher activity than commercial Amoxicillin against gram-positive *s. aureus* bacteria and moderate activity against *C.albicans* fungi.[26] The activity of compounds was increased with the increase of hydrophilicity and aromaticity of the compounds. Heteroatoms and halogens were helpful in the activity of the compounds, and they were found to be the most potent antimicrobial.[27] Halogen atoms increase the molecule's lipophilicity, which expedites molecule distribution across membranes. It also facilitates hydrophobic interactions between compounds and specific binding sites on receptors or enzymes.[28] Additionally, Schiff bases find extensive use in dyes [29, 30] as an organic synthesis catalyst [31] as polymer stabilizers.[32] Moreover, it has been demonstrated that Schiff bases can act as plant growth regulators.[33] The development of novel antibiotics against gram-positive and gram-negative bacteria was a challenge, and their discovery led to the achievements of modern science by decreasing bacterial infection. Amoxicillin, Norfloxacin, Chloramphenicol, and Ciprofloxacin are the most common antibiotics for these bacterial infections. However, they have neurological alterations and side effects due to drug interaction with the central nervous system.[34] Therefore, finding new alternative antibiotics with ease of synthesis and relatively fewer side effects is essential.[35] Considering the therapeutic potential of the above organic compounds, Schiff bases of 2, 5-dihydroxybenzaldehyde were synthesized, characterized, and examined for their antibacterial and antifungal activities. The main intention of the present work was to explore the essential characteristics of these Schiff bases in terms of their applications as valuable drugs.

2. Experimental

2.1. Materials and instrumentation.

The chemicals and solvents were of commercial-grade quality. The SHIMADZU FT-IR-8400 spectrometer with KBr pellets was used to capture FT-IR spectra. BRUKER AVANCE III (500MHz) spectrometer was used for recording the ^{1}H-NMR and ^{13}C-NMR spectra of compounds in $CDCl_3$. Proton chemical shifts were measured in ppm with respect to tetramethyl silane, which served as an internal standard. ESI-MS spectra of compounds have been carried out with waters, micro mass Q-Tof micro instrument. E-Merck pre-coated silica gel plates were used for thin-layer chromatography (TLC) to monitor the advancement of all

reactions. The plates were visualized with a UV-Visible cabinet. A single crystal X-ray diffraction study was conducted at IIT Madras (India).

2.2- General procedure for preparation of Schiff bases.

All the compounds were synthesized by reacting equimolar quantities of aldehyde and amine. A hot methanolic solution of 2, 5-dihydroxybenzaldehyde (1mmol) was added dropwise to the hot methanolic solution of primary amine (1mmol). The resulting reaction mixture was refluxed for 2–3 hours, during which TLC monitored the reaction. The resultant colored solid was collected, washed with cold methanol, and recrystallized in an appropriate solvent [7, 36, 37]

2.2.1 S_1: (Z)-2-((4-Bromo-3-chlorophenylimino) methyl) benzene-1, 4-diol.

Red Crystals, Yield 92%, MP: 225°C. ^{1}H-NMR (DMSO, 500MHz) (δ, ppm): 6.82–6.80 (d, 1H, Ar-H); 6.91–6.89 (dd, 1H, Ar-H); 7.07–7.06 (d, 1H, Ar-H); 7.31–7.29 (dd, 1H, Ar-H); 7.70 (d, 1H, Ar-H); 7.81–7.79 (d, 1H, Ar-H); 8.88 (s, 1H, HC = N); 9.13 (s, 1H, -OH); 11.73 (s, 1H,-OH).ESI-MS: 327.96 (Obs); 326.5 (Cal). ^{13}C-NMR ($CDCl_3$, 500 MHz) (δ, ppm): 164.43; 153.0; 149.63; 149.33;134.21; 133.75; 122.83; 122.26; 121.72; 119.14; 118.68; 117.23; 116.62; FT-IR (KBr pallete, cm^{-1}): 3296 (OH); 1621 (C = N); 1591(C = C); 1209(C-O).

2.2.2 S_2: (Z)-2-((4-cyclohexylphenylimino) methyl) benzene-1, 4-diol.

Red, solid, Yield-85%, MP-159°C. ^{1}H-NMR (DMSO, 500MHz) (δ, ppm): 1.26–1.22 (m, 1H, -CH); 1.44–1.32 (m, 4H, -CH); 1.71–1.68 (m, 1H, -CH); 1.79–1.77 (m,4H, -CH); 2.53–2.49 (m,1H, -CH); 6.80 (dd, 1H, Ar-H); 6.87–6.85 (dd, 1H, Ar-H); 7.03–7.02 (1H,d,Ar-H); 7.31–7.27 (d, 1H, Ar-H); 8.83 (s, 1H, -HC = N), 9.07 (s,1H,-OH), 12.39 (s, 1H, OH). ESI-MS: 295.38 (Obs), 295.16 (Cal). ^{13}C-NMR (DMSO,500 MHz) (δ, ppm): 162.32, 153, 149.51, 146.35, 146.04; 172; 121.14; 120.78; 119.21; 117; 116.86; 43.27; 33.86; 26.24; and 25.47. FT-IR (KBr pallete, cm^{-1}): 3285 (OH); 2924 (OH); 1611 (C = N); 1577 (C = C); 1218 (C-O).

2.2.3 S_3: (E)-2-((1-methyl-1H-benzo[d]imidazol-2-yliminoimidazol-2-ylimino)methyl) benzene-1, 4-diol.

Turmeric Yellow crystals, Yield-86%, MP-262°C. ^{1}H-NMR ($CDCl_3$,500 MHz) (δ, ppm):3.85 (s, 3H,-CH_3); 6.88–6.87 (d, 1H, Ar-H); 6.97–6.95 (dd, 1H, Ar-H); 7.25–7.21(m, 2H, Ar-H); 7.37–7.36 (d, 1H, Ar-H); 7.55–7.54 (dd, 1H, Ar-H); 7.6–7.59 (dd, 1H, Ar-H); 9.2 (s, 1H, -OH); 9.63 (s, 1H, HC = N); 10.87(s, 1H, -OH). ESI-MS: 268.11 (Obs); 267.10 (Cal). ^{13}C-NMR ($CDCl_3$, 500MHz) (δ, ppm): 163.88; 154.11; 153.43; 149.98; 141.13; 135.39; 123.06; 122.99,121.89; 120.15; 118.51; 117.55; 114.59; 110.06; 28.72. FT-IR (KBr pallete, cm^{-1}): 3058 (OH); 1616 (C = N); 1573 (C = C); 1223 (C-O).

2.2.4 S_4: 2-((E)-(quinolin-3-ylimino) methyl) benzene-1, 4-diol.

Reddish brown crystals, Yield-91%, MP: 239°C, ^{1}H-NMR (DMSO,500 MHz) (δ, ppm): 6.87–6.85(d, 1H, Ar-H); 6.94 (dd, 1H, Ar-H); 7.14 (d, 1H, Ar-H); 7.66–7.63 (dd, 1H, Ar-H); 7.76–7.73 (m, 1H, Ar-H); 8.03–8.01(d, 1H, Ar-H); 8.07–8.05 (d, 1H, Ar-H); 8.33–8.32 (d,1H, Ar-H); 9.01 (d, 1H, Ar-H); 9.08 (s, 1H, -OH); 9.17 (s, 1H, -HC = N); 11.86 (s,1H, -OH). ESI-MS: 265.10 (Obs); 264.28(Cal).^{13}C-NMR (DMSO,500MHz) (δ, ppm): 164.69; 153; 149.68; 146.63; 146.17; 141.98; 128.93; 128.64; 128.14; 127.88; 127.12; 124.64; 121.65; 119.47; 117.29; 116.44. FT-IR (KBr pallete, cm^{-1}): 3431 (OH); 3053 (OH); 1625 (C = N); 1579 (C = C); 1233 (C-O).

2.2.5 S_5: 2-((E)-(2-methyl-5-nitrophenylimino) methyl) benzene-1, 4-diol.

Yellow crystals, Yield-93%, MP: 213°C. ^{1}H-NMR (DMSO,500MHz) (δ, ppm): 2.42 (s, 3H, Ar-CH_3); 6.84–6.82 (d,1H, Ar-H); 6.92–6.90 (dd, 1H, Ar-H); 7.59–7.57(d, 1H, Ar-H); 8.06–8.04 (dd, 1H, Ar-H); 8.14–8.13(d,1H, Ar-H); 8.90 (s,1H,-HC = N); 9.14 (s,1H, -OH); 11.84 (s,1H, OH).ESI-MS: 273.09 (Obs); 272.26 (Cal).^{13}C-NMR (DMSO,500MHz) (δ, ppm): 164.57; 153.07; 149.64; 148.52; 146.71; 140.06; 131.28; 121.76; 120.61; 119.32; 117.19; 116.67; 112.82; FT-IR (KBr pallet,cm^{-1}): 3467 (OH); 1621 (C = N); 1582 (C = C); 1202 (C-O).

2.2.6 S_6: 2-((E)-(cycloheptylimino) methyl) benzene-1, 4-diol.

Yellow crystals, Yield-93%, MP: 140°C. ^{1}H-NMR (DMSO,500 MHz) (δ, ppm): 1.52–1.47 (m, 2H, -CH); 1.58–1.53 (m,4H, -CH); 1.70–1.60 (m, 4H, -CH); 1.81–1.76 (m, 2H, -CH); 3.47–3.42 (m, 1H, -CH); 6.69–6.67 (d, 1H, Ar-H); 6.76 (dd, 1H, Ar-H); 6.78 (d, 1H, Ar-H); 8.41 (s,1H,HC = N); 8.92 (s,1H,-OH); 12.82 (s,1H,-OH). ESI-MS: 234.15 (Obs); 233.31(Cal). ^{13}C-NMR (DMSO, 500MHz) (δ, ppm):162.60; 152.92; 149.10; 119.41; 118.51; 116.59; 116.34; 68.68; 40.01; 35.85; 27.84; 23.5. FT-IR (KBr pallete, cm^1): 3405 (OH); 1640 (C = N); 1159(C-O).

2.2.7 S_7: 2-((E)-(2,6-difluorophenylimino)methyl)benzene-1,4-diol.

Red crystals, Yield-93%, MP: 221°C. ^{1}H-NMR (DMSO, 500MHz) (δ, ppm): 6.88 (d, 1H, Ar-H); 6.97 (dd, 1H, Ar-H); 7.15 (d, 1H, Ar-H); 7.31(m, 3H, Ar-H); 8.94 (s, 1H, -HC = N); 9.18 (s, 1H, OH); 11.43 (s, 1H, OH). ESI-MS: 250.07 (Obs); 249.06 (Cal).^{13}C-NMR (DMSO,500MHz) (δ, ppm): 168.51; 155.76; 153.79; 153.01; 149.87; 126.62; 122.28; 119.53; 117.57; 115.87; 112.37. FT-IR (KBr pallete, cm^{-1}): 3307 (OH); 1621 (C = N); 1580 (C = C); 1167(C-O).

2.2.8 S_8: 2-((E)-(5-methylthiazol-2-ylimino) methyl) benzene-1, 4-diol.

Yellow crystals, Yieid-84%, MP: 245°C. ^{1}H-NMR (DMSO, 500MHz) (δ, ppm): 2.45 (s, 3H, Ar-CH_3); 6.84–6.82(d, 1H, Ar-H); 6.93–6.90 (dd,1H, Ar-H); 7.21–7.20 (d,1H, Ar-H); 7.41 (d,1H, Ar-H); 9.13(s,1H, -HC = N); 9.14 (s,1H, -OH);10.76(s,1H, -OH). ESI-MS: 235.05 (Obs); 234.27(Cal). ^{13}C-NMR (DMSO, 500MHz) (δ, ppm):169.12; 161.61; 153.01; 149.93; 138.94; 132.80; 122.69; 119.63; 117.48; 114.53; 12.02. FT-IR (KBr pallete, cm^{-1}): 3053(OH); 1614 (C = N); 1576 (C = C); 1216 (C-O).

2.3. Single Crystal X-ray Diffraction-

Crystal evaluation and data collection of compound S_1 were performed on a BRUKER AVANCE III diffractometer with M_oK_α radiation (I = 0.71073). Reflections were collected at different starting angles, and the APEXII program suite was used to index the reflections. The structure was solved by the direct method using the SHELXS.[38] The crystallographic, structure refinement parameters, bond length, bond angles, and hydrogen bonding for the compound are given in Table 3–5, and Crystal Structure and packing diagrams are represented in Figs. 3–4.

2.4. *In vitro* Antimicrobial Activity.

The broth dilution method was used to evaluate the antimicrobial activity. It is one of the non-automated *in vitro* bacterial susceptibility tests. This classic method yields a quantitative result for the number of antimicrobial agents needed to inhibit specific microorganisms' growth. The Mueller Hinton broth was used as a nutrient medium to grow and dilute the drug suspension for the test bacteria. The inoculum size for the test strain was adjusted to 10^8cfu [colony forming unit] per milliliter by comparing the turbidity. DMSO was used as a diluent to get the desired concentration of drugs to test upon standard bacterial strains. Serial dilutions were prepared in primary and secondary screening. The control tube containing no antibiotic is immediately subcultured by spreading a lapful evenly over a quarter of a plate of medium suitable for the growth of the test organism and put for incubation at 37°C overnight. The tubes are then incubated overnight. The MIC of the control organism is read to check the accuracy of the drug concentrations. The lowest concentration inhibiting the organism's growth is recorded as the MIC. The amount of growth from the control tube before incubation is compared. Each synthesized drug was diluted, obtaining 2000 µg/ml concentration as a stock solution. In primary screening, 1000 µg/ml, 500 µg/ml, and 250 µg/ml concentrations of the synthesized drugs were taken for the test. The active synthesized drugs found in this primary screening were further tested in the second set of dilutions against all microorganisms. In the secondary screen, drugs found involved in preliminary screening were similarly diluted to obtain 200 µg/ml, 100 µg/ml, 50 µg/ml, 25 µg/ml, 12.5 µg/ml, and 6.250 µg/ml concentrations. The highest dilution showing at least 99% inhibition zone is taken as MIC. The result of this is much affected by the size of the inoculums. The test mixture should contain 10^8 organisms/ml. [39–41]

2.5. Molecular Docking study-

The molecular docking Glide module (Schrodinger Inc., USA) has been used for ligand docking against the β-ketoacyl-ACP-synthase-I. The X-ray crystallographic structure of β-ketoacyl-acyl carrier protein ACP

syntheses-I receptor was retrieved from the protein data bank, with accession ID 1FJ4. The “protein preparation wizard” panel prepared the retrieved protein structure. Using prime during the stages of pr-processing, bond ordering was assigned, missing hydrogen was added, disulfide bonds were formed, and missing side chains and loops were modified. In the final refinement stage, the OPLS3 force field reached complete energetic optimization, with the RMSD of heavy atoms set to 0.3 Å. The Lig Prep panel prepared all the synthesized compounds' 3D structures. The ionization state of each structure was established at a physiological pH of 7.2 ± 0.2. The active side grid was assigned by centralizing the cognate ligand in the crystal structure and using the default box dimension. Finally, the molecular docking study was carried out using Schrodinger's glide. The ready minimum energy 3D structure of the ligands and the receptor grid file were loaded into Maestro's work area, and the ligands were docked using extra precision (SP) docking methodology. [42–44]

3. Result And Discussion

3.1. Chemistry.

Schiff bases (S_1-S_8) were prepared by condensing 2,5-dihydroxybenzaldehyde with substituted amines in methanol. **(Scheme.1)** all synthesized compounds were recrystallized from methanol, monitored for their purity by TLC, and characterized by FT-IR, ^{1}H-NMR, ^{13C}-NMR, and ESI-MS. X-ray diffraction technique was used to the determined structure of S_1, one of the compounds of the series.

3.2. Reagents and conditions.

Scheme.1 shows the synthesis of azomethines, confirmed by FT-IR, ^{1}H-NMR, ^{13}C-NMR, and ESI-MS. The series of ligands can be divided into three major groups.

Azomethine N is bonded to non-conjugated cycloheptane (S_6) and cyclohexane *via* benzene ring (S_2); Azomethine N bonded to conjugated benzene with electron withdrawing and electron donating substituent.

3.3. IR-Spectroscopy.

The IR spectra of the ligands have been summarized in Table 1. The absence of the aldehydic carbonyl stretching bands, twin peaks of -NH_2 (~ 2850–2900 cm^{-1}) of substituted primary amines, and the appearance of the characteristic azomethine $v_{C=N}$ bands at 1600 cm^{-1} confirmed the formation of the Schiff bases. The broadness of the v_{OH} band at 3450 cm^{-1} may be attributed to the intramolecular hydrogen bond between CH = $N_{(imine\ nitrogen)}$ and $OH_{(phenolic)}$ [45, 46]. The positions and shapes of a few basic FT-IR bands of the free ligands (S_1–S_8) are compared in Table 1. It is clear from the spectral data that the assigned bands for the v CH = N and C-O in the ligands, located at 1640 – 1614 $cm^{-1}$and 1235–1267 $cm^{-1,}$ respectively, both suffer from reduced intensity and wave numbers, indicating an electron-donating and electron-withdrawing effect from the amine moiety substituent.[47] This is reflected in the

IR bands of the azomethine in the Schiff bases S_1, S_5, and S_7, which observe an electron-withdrawing effect due to the presence of $-NO_2$ and –X substituent on the adjacent aromatic ring. On the other hand, the azomethine IR band in S_3, S_8, and S_2 shifted to a lower frequency due to the electron-donating effect of heterocyclic adjacent rings.[48] (Table 1) alternatively, the azomethine IR band is observed to be shifted to a higher frequency in S_5 & S_7, which can be attributed to the electron-withdrawing halogen and nitro substituents. It has been reported that Schiff bases with halogen substituents to the aromatic ring of the N-benzylidene alanine methyl ester substrate are desired to increase its enantioselectivity during the alkylation process, with a para-chloro substituent producing favorable outcomes.[49] Thus, the variation due to electron-withdrawing and electron-donating substituents is essential to tune the properties of these compounds for various applications of these ligands. [50, 51]

3.4. ^{1}H-NMR and ^{13}C-NMR Spectroscopy

^{1}H-NMR and ^{13}C-NMR are additional techniques that support the structure elucidation of the synthesized compounds. For a discussion of the ^{1}H-NMR and ^{13}C-NMR spectra, it is suitable to show the numbering used for these compounds, viz, (Fig. 1)

The NMR data are collected in Fig. 2 and the supplementary information with detailed assignments on each designated structure. The below figure presents part of the ^{1}H-NMR spectra of S_1-S_8 ligands arranged to show the trend in the proton signals. Regarding the fundamental ^{1}H-NMR peaks, the phenolic OH of the two phenolic groups in the range δ 9.55–9.66 ppm and δ 11.50–12.50 ppm were shown. The azomethine protons were observed as a singlet at δ 8.46–8.80 ppm. The ortho-OH of the ligands showed a systematic shift with respect to the substituent's electron-withdrawing and electron-donating nature. Figure 2 shows the ^{1}H-NMR spectra arranged to view the increasing chemical shift of –OH. These findings coincide with the conclusions drawn from IR spectral studies.

In ^{13}C-NMR of all compounds, remarkable imine carbon (C = N) peaks were δ 157.82–162.11 ppm (Table 2). In ^{13}C-NMR of all compounds, outstanding iminic carbon (C = N) peaks were in the δ 162.3–169.11 ppm range. The spectral data of other aromatic protons are under the structures of anticipated compounds. The aldimine π-bond disruption is primarily responsible for the ^{13}C-NMR changes. It is essentially a second-order effect when the effect is extended to the methine protons. Effects of substitutes on ^{13}C-NMR: i) on δ C-1': We observed the typical effects of electron-withdrawing and electron-releasing groups. A shift range of 68 δ ppm for non-conjugated cycloheptane substituent in S_5, approximately 146 δ ppm for aromatic rings in S_2, and 161.61 δ ppm for heterocyclic thiazole substituent in S_8 is seen for δC-1, where the effect of the substituent is most excellent. ii) On δ C-6: Values do not really depend on the substituent impact. iii) On δ C-α: Similar chemical shifts were found when the correlations relating to δ C-α were compared to other findings in the literature, taking the effects of electronics into account.[52] However, S_7 recorded the most significant shift of 169.11, explained by two fluorides in the aromatic ring next to the azomethine carbon. On δ C-1 and C4: It was discovered that these diol carbons were least affected and δC-6 also showed only slight CMR alterations. Recently, our

team has reported similar CMR alterations for δ C-α. These outcomes are consistent with the in-depth analysis, where substantial linear and bilinear correlations for imine carbon were seen, demonstrating a resonance effect on chemical changes [52].

The mass spectra of the compounds displayed base peaks at M^+ and M^{+1} corresponding to their respective molecular weight. However, the halide effect in the mass spectra was observed in the ESI-MS of S_1 and found two peaks (327.96 and 329.96) separated by two m/z units and with a ratio of 3:1 in the peak heights, that confirms the molecule contains one chlorine atom. The ratio of the two isotopes of bromine, ^{79}Br, and ^{81}Br, is roughly 1:1. The ESI-M of S_1 produced peaks at 325.96 and 327.96 that were separated by two m/z units and had a peak height ratio of 1:1. This confirmed one bromine substituent in S_1

3.5. X-Ray crystallographic analysis.

The crystal of Schiff base (S_1) for X-ray crystallographic analysis was grown by the slow evaporation method in acetonitrile solvent at room temperature. A suitable single crystal was selected for X-ray diffraction analysis and was mounted on a Bruker Apex II CCD diffractometer. The crystal was kept at 298 (2) K during the investigation. The crystal system and refinement parameters are shown in Table 3. A perspective diagram of S_1 is shown in Figs. 3 and 4. The bond length and angles agree with standard values; the list of selected bond lengths and angles is given in Table 4. The crystal structure of the Schiff base represented C (2)-Cl (1) and C (3)-Br (1) distances at 1.727 (2) Å and 1.886 (2) Å, respectively. Single bond distance C (6)-N (1) distances at 1.412(3) Å. Whereas (C = N) C (7)-N (1) distance at 1.285(3). The two C (10)-O (2) and C (13)-O (1) have bond distances at 1.368(3) and 1.352(3) Å. The C (7)-H (7) (H-C = N) distance is 0.93Å. In the crystal, two types of intermolecular hydrogen bonding interactions are present. (Table 5**)** The intense primary O (1)-H (1A)...N (1) intramolecular hydrogen between the hydroxyl group and nitrogen of -C = N group and secondary weak intermolecular H-bonding C (11)-H (11)...Cl (1) #1 and O (2)-H (2A)...O (1) #2 interactions.

3.6. Biological assay.

3.6.1. Antibacterial activity.

The compounds (S_1-S_8) were tested for their antibacterial activity against two gram-positive *S. aureus*, *S. pyogenes*, and two gram-negative *E. coli* and *P. aeruginosa*. *E. coli* causes food poisoning, *S. aureus* causes various colic diseases and throat infections, *P. aeruginosa*, is usually responsible for a blood infection, infects the urinary tract and pulmonary tract, and involves other blood infections.[53] *S. pyogenes* causes frequent throat and skin infections, invasive diseases such as arthritis, and streptococcal toxic shock syndrome.[54] Compounds S_3 and S_6 Showed significantly potent activity against *E. coli* (50-62.5 µg/mL), while compounds S_1, S_2, and S_8 exhibited excellent activity (100 µg/mL). **(**Table 6**)** Compounds S_3 and S_7 showed significant activity against *P. aeruginosa* (100 µg/mL), while compounds S_1, S_2, S_5, S_6, and S_8 exhibited good activity (125 µg/mL). Compound S_6 shows potent

activity against *S. aureus* (62.5µg/mL) while compound S_1, S_2, S_3, S_5 exhibited well to moderate activity (100–125µg/mL).Compounds S_3 and S_5 exhibited potent activity against *S. pyogenes* while compounds S_8 and S_7 exhibited moderate activity (100–125µg/mL). It is observed that, S_4 found to be weak against all bacterial strains but good activity against *S. aureus.*

3.6.2. Antifungal activity.

Synthesized Schiff base ligands have been evaluated in *vitro* against three different fungi viz *C. albicans, A. niger*, and *A. clavatus* and compared with standard drugs Griseofulvin **(**Table 6**).** The result of antifungal screening showed that Schiff bases S_1, S_5, S_6, S_7, and S_8 (100–250 µg/ml) had shown excellent potency against *C. albicans* compared to standard drugs. Schiff base S_1, S_5, S_6, and S_7 have also exhibited inhibition of fungal species *A. Niger;* however, it is lesser than standard drugs. Only compound S_5 showed weak inhibition against *A. clavatus*.

3.6.3. Structural activity relationship (SAR).

Schiff base derivatives S_3 exhibited the best activity for all strains; this observation indicated that a heterocyclic ring containing an N atom and methyl group or adding a benzimidazole ring increases antibacterial activity [55, 56]. One more fact is that adding an aromatic ring increases the lipophilicity of the drug, which should increase its penetration into the bacterial cell membrane.[57] The difference in the activity against various strains depends either on the impermeability of the cells of the microbes or differences in the ribosome of microbial cells [9, 25, 58]. A comprehensive SAR study shows that electron-withdrawing groups such as -Cl, -Br, -NO_2, -F will moderate the antibacterial activity of strains.[59, 60] Schiff base S_4 containing quinoline heterocycle decreases the antibacterial activity but shows moderate activity against *S. aureus*. However, in our previous research group, quinoline substituents with thymoladehyde have shown optimum activity against *S. aureus*.[61] Electron-donating cycloheptane ring increases activity. Interestingly, we observed that compound S_3 containing benzimidazole ring has potent antibacterial activity but does not have antifungal activity against all fungal strains; Sharma et al. has been reported that the addition of benzimidazole ring markedly enhanced the antibacterial potential against *E.coli* and declined antifungal activity.[56] S_5 has well to moderate fungal inhibition against all strains, possibly due to the electron-withdrawing -NO_2 group. Similarly, compound S_4 has very weak inhibition against all fungal strains. It may be due to N-containing heterocycles decreasing antifungal activity, considering the common point of S_3 and S_4 is to have N-containing heterocycles. The presence of an electron-withdrawing group increases antifungal activity.[62]

3.6.4 Molecular docking.

The β-ketoacyl-ACP synthase-I is the vital regulator of type II fatty acid synthesis. Fatty acid synthesis has emerged as a promising target for developing novel therapeutic agents. Lipid synthesis is essential for cell viability. However, specificity for bacteria and other infectious organisms can be achieved by utilizing the organizational and structural differences in different organisms' fatty acid synthetic systems. The β-ketoacyl-ACP synthase-I is the most extensively studied target in *E. coli* and has emerged as an essential

regulator of the initiation and elongation steps in fatty acid synthesis. These enzymes catalyze the Claisen condensation reaction, transferring an acyl primer to malonyl-ACP and creating a β-ketoacyl-ACP lengthened by two carbon units.[63] A docking study has been performed by SP-docking mode. Among the synthesized compounds, S_4 (-6.785) and S_3 (-6.59) showed more significant docking scores than Ampicillin (– 7.33) (Table 7). Compound S_4 showed the hydrogen bond interaction with the GLY 205 and VAL 270 of Beta-ketoacyl-ACP synthase-I via the phenolic hydroxyl group. **(**Fig. 5**)** Compound S_3 showed two hydrogen bond interactions with VAL 304 and MET 204 via a phenolic ring similar to compound S_4. **(**Fig. 6**)** Docking interactions were compared with Ampicillin. **(**Fig. 7**)** These both the compounds occupy the same binding site where Ampicillin is binding but interacts with different amino acids in the binding site cavity of the Beta-ketoacyl-ACP synthase-I; this result indicates that these compounds could also be effective against the resistance β-ketoacyl-ACP synthase-I of *E.coli*.

4. Conclusion

The present study reveals that the novel 2, 5-dihydroxybenzaldehyde-based Schiff bases exhibit potent antifungal and antibacterial activity. *In vitro* and *in silico* studies showed compound S_3 is a promising antibacterial therapeutics agent against all bacterial strains. Schiff base S_8 has superior antifungal activity against *C. albicans* compared to standard drugs. The molecular docking result indicates these compounds could also be effective against the resistance β-ketoacyl-ACP synthase-I of *E.Coli*. Here, preliminary structure-activity relationships and molecular modeling research have provided new information about how a macromolecular enzyme interacts with its inhibitor ligands. Thus, it represents a promising motif as an antibacterial drug.

Declarations

Acknowledgment.

The authors thank the honorable Management, Principal Dr. Gotan Jain, KKHA arts, SMGL Commerce, and SPHJ Science College Chandwad for providing research facilities.

Ethical Approval Not applicable.

Competing interests The authors declare that they have no known competing financial interests or personal relationships that could have appeared to influence the work reported in this paper.

Author’s contributions

All mentioned authors have contributed to this research work.

Funding Not Applicable

Avaibility of data and Materials

All data generated or analyzed during this study are included in this published article and upon request data can be available from the corresponding author on reasonable request.

Supplementary data.

CCDC number 2208358 contains the supplementary crystallographic data for this paper. This data can be obtained free of charge via https://www.ccdc.cam.ac.uk/data_request/CIF, by emailing at data_request@ccdc.cam.ac.uk, or by contacting Cambridge Crystallographic Data Centre, 12 Union Road, Cambridge CB21EZ, UK; fax: +44 1223 336033. Crystallographic details and FT-IR, ^{1}H-NMR and ^{13}C-NMR, mass spectra, and theoretical simulation tables are also included in supplementary data.

References

1. C. Nathan, Nature **431**, 899 (2004).
2. K. Cheng, Q.-Z. Zheng, Y. Qian, L. Shi, J. Zhao, and H.-L. Zhu, Bioorg. Med. Chem. **17**, 7861 (2009).
3. J. Wang, S. M. Soisson, K. Young, W. Shoop, S. Kodali, A. Galgoci, R. Painter, G. Parthasarathy, Y. S. Tang, R. Cummings, S. Ha, K. Dorso, M. Motyl, H. Jayasuriya, J. Ondeyka, K. Herath, C. Zhang, L. Hernandez, J. Allocco, Á. Basilio, J. R. Tormo, O. Genilloud, F. Vicente, F. Pelaez, L. Colwell, S. H. Lee, B. Michael, T. Felcetto, C. Gill, L. L. Silver, J. D. Hermes, K. Bartizal, J. Barrett, D. Schmatz, J. W. Becker, D. Cully, and S. B. Singh, Nature **441**, 358 (2006).
4. S. W. Nowotarska, K. Nowotarski, I. R. Grant, C. T. Elliott, M. Friedman, and C. Situ, Foods **6**, (2017).
5. A. Schabauer, C. Zutz, B. Lung, M. Wagner, and K. Rychli, Front. Vet. Sci. **5**, (2018).
6. Wong Stella Y. Y., Grant Irene R., Friedman Mendel, Elliott Christopher T., and Situ Chen, Appl. Environ. Microbiol. **74**, 5986 (2008).
7. S. Murtaza, A. Abbas, K. Iftikhar, S. Shamim, M. S. Akhtar, Z. Razzaq, K. Naseem, and A. M. Elgorban, Med. Chem. Res. **25**, 2860 (2016).
8. A. Shirwaikar, S. Malini, and S. C. Kumari, (2003).
9. Y. Bayeh, F. Mohammed, M. Gebrezgiabher, F. Elemo, M. Getachew, and M. Thomas, Adv. Biol. Chem. **10**, 127 (2020).
10. E. S. Harpstrite, D. S. Collins, A. Oksman, E. D. Goldberg, and V. Sharma, Med. Chem. **4**, 392 (2008).
11. A. Catalano, M. S. Sinicropi, D. Iacopetta, J. Ceramella, A. Mariconda, C. Rosano, E. Scali, C. Saturnino, and P. Longo, Appl. Sci. **11**, (2021).
12. M. S. Alam, J.-H. Choi, and D.-U. Lee, Bioorg. Med. Chem. **20**, 4103 (2012).
13. H. Wang, H. Yuan, S. Li, Z. Li, and M. Jiang, Bioorg. Med. Chem. Lett. **26**, 809 (2016).
14. J. Cheng, K. Wei, X. Ma, X. Zhou, and H. Xiang, J. Phys. Chem. C **117**, 16552 (2013).
15. S. Sehrawat, N. Sandhu, V. Anand, S. K. Pandey, A. Sharma, R. K. Yadav, A. P. Singh, and A. P. Singh, J. Mol. Struct. **1269**, 133782 (2022).

16. N. Uddin, F. Rashid, S. Ali, S. A. Tirmizi, I. Ahmad, S. Zaib, M. Zubair, P. L. Diaconescu, M. N. Tahir, J. Iqbal, and A. Haider, J. Biomol. Struct. Dyn. **38**, 3246 (2020).
17. S. Alyar, Ü. Ö. Özmen, Ş. Adem, H. Alyar, E. Bilen, and K. Kaya, J. Mol. Struct. **1223**, 128911 (2021).
18. M. Elhag, H. E. Abdelwahab, M. A. Mostafa, G. A. Yacout, A. Z. Nasr, P. Dambruoso, and M. M. El Sadek, Int. J. Biol. Macromol. **184**, 558 (2021).
19. N. Yuldasheva, N. Acikyildiz, M. Akyuz, L. Yabo-Dambagi, T. Aydin, A. Cakir, and C. Kazaz, J. Mol. Struct. **1270**, 133883 (2022).
20. V. A. G. L. Balaji G. Sujatha, Eur. J. Mol. Clin. Med. **7**, 1760 (2020).
21. A. Sakthivel, K. Jeyasubramanian, B. Thangagiri, and J. D. Raja, J. Mol. Struct. **1222**, 128885 (2020).
22. S. J. Kirubavathy, R. Velmurugan, R. Karvembu, N. S. P. Bhuvanesh, I. V. M. V. Enoch, P. M. Selvakumar, D. Premnath, and S. Chitra, J. Mol. Struct. **1127**, 345 (2017).
23. S. Slassi, M. Aarjane, K. Yamni, and A. Amine, J. Mol. Struct. **1197**, 547 (2019).
24. M. Taha, N. H. Ismail, W. Jamil, H. Rashwan, S. M. Kashif, A. A. Sain, M. I. Adenan, E. H. Anouar, M. Ali, F. Rahim, and K. M. Khan, Eur. J. Med. Chem. **84**, 731 (2014).
25. A. A. Shanty, J. E. Philip, E. J. Sneha, M. R. Prathapachandra Kurup, S. Balachandran, and P. V. Mohanan, Bioorganic Chem. **70**, 67 (2017).
26. K. J. Rajimon, N. Elangovan, A. Amir Khairbek, and R. Thomas, J. Mol. Liq. **370**, 121055 (2022).
27. L. Shi, H.-M. Ge, S.-H. Tan, H.-Q. Li, Y.-C. Song, H.-L. Zhu, and R.-X. Tan, Eur. J. Med. Chem. **42**, 558 (2007).
28. C. T. Prabhakara, S. A. Patil, S. S. Toragalmath, S. M. Kinnal, and P. S. Badami, J. Photochem. Photobiol. B **157**, 1 (2016).
29. R. A. Ahmadi and S. Amani, Molecules **17**, 6434 (2012).
30. D. A. Safin, M. G. Babashkina, M. Bolte, A. L. Ptaszek, M. Kukułka, and M. P. Mitoraj, J. Lumin. **238**, 118264 (2021).
31. M. F. I. Al-Hussein and M. S. S. Adam, Appl. Organomet. Chem. **34**, e5598 (2020).
32. D. S. Ahmed, M. Kadhom, A. G. Hadi, M. Bufaroosha, N. Salih, W. H. Al-Dahhan, and E. Yousif, Chemistry **3**, 288 (2021).
33. G. N. Naik, R. P. Bakale, A. H. Pathan, S. G. Ligade, S. A. Desai, and K. B. Gudasi, J. Chem. **2013**, 810892 (2012).
34. H. Sternbach and R. State, Harv. Rev. Psychiatry **5**, (1997).
35. S. A. Khan, A. M. Asiri, A. A. Basheike, and K. Sharma, Eur. J. Chem. **4**, 454 (2013).
36. A. Cinarli, D. Gürbüz, A. Tavman, and A. S. Birteksöz, Chin. J. Chem. **30**, 449 (2012).
37. D. Gürbüz, A. Cinarli, A. Tavman, and A. S. Birteks?z, Chin. J. Chem. **30**, 970 (2012).
38. J. C. Ezeorah, V. Ossai, L. N. Obasi, M. I. Elzagheid, L. Rhyman, M. Lutter, K. Jurkschat, N. Dege, and P. Ramasami, J. Mol. Struct. **1152**, 21 (2018).
39. S. K. Tadavi, A. A. Yadav, and R. S. Bendre, J. Mol. Struct. **1152**, 223 (2018).

40. A. W. BAUER, D. M. PERRY, and W. M. M. KIRBY, AMA Arch. Intern. Med. **104**, 208 (1959).
41. M. Shebl, Spectrochim. Acta. A. Mol. Biomol. Spectrosc. **117**, 127 (2014).
42. R. Girase, I. Ahmad, R. Pawara, and H. Patel, SAR QSAR Environ. Res. **33**, 215 (2022).
43. I. Ahmad, R. H. Pawara, R. T. Girase, A. Y. Pathan, V. R. Jagatap, N. Desai, Y. O. Ayipo, S. J. Surana, and H. Patel, ACS Omega **7**, 21820 (2022).
44. I. Ahmad, M. Shaikh, S. Surana, A. Ghosh, and H. Patel, J. Biomol. Struct. Dyn. **40**, 3046 (2022).
45. A. Golcu, M. Tumer, H. Demirelli, and R. A. Wheatley, Inorganica Chim. Acta **358**, 1785 (2005).
46. S. M. Ben-saber, A. A. Maihub, S. S. Hudere, and M. M. El-ajaily, Microchem. J. **81**, 191 (2005).
47. M. Sahin, N. Kocak, U. Arslan, O. Sahin, and M. Yilmaz, J. Macromol. Sci. Part A **50**, 821 (2013).
48. H. Szatylowicz, O. A. Stasyuk, and T. M. Krygowski, in *Adv. Heterocycl. Chem.*, edited by E. F. V. Scriven and C. A. Ramsden (Academic Press, 2015), pp. 137–192.
49. M. J. O'Donnell, M. D. Drew, J. T. Cooper, F. Delgado, and C. Zhou, J. Am. Chem. Soc. **124**, 9348 (2002).
50. C. Cativiela and J. I. Garcia, Can. J. Chem. **68**, 1477 (1990).
51. B. Sreenivasulu, F. Zhao, S. Gao, and J. J. Vittal, Eur. J. Inorg. Chem. **2006**, 2656 (2006).
52. A. Echevarria, M. da G. Nascimento, V. Gerônimo, J. Miller, and A. Giesbrecht, J. Braz. Chem. Soc. **10**, 60 (1999).
53. M. S. Akhtar, A. Ismail, S. Murtaza, M. N. Tahir, S. Shamim, and U. A. Rana, J. Chem. Soc. Pak. **38**, 242 (2016).
54. Luca-Harari Bogdan, Darenberg Jessica, Neal Shona, Siljander Tuula, Strakova Lenka, Tanna Asha, Creti Roberta, Ekelund Kim, Koliou Maria, Tassios Panayotis T., van der Linden Mark, Straut Monica, Vuopio-Varkila Jaana, Bouvet Anne, Efstratiou Androulla, Schalén Claes, Henriques-Normark Birgitta, and Jasir Aftab, J. Clin. Microbiol. **47**, 1155 (2009).
55. V. Pandey, V. Chawla, and S. K. Saraf, Med. Chem. Res. **21**, 844 (2012).
56. U. K. Sharma, S. Sood, N. Sharma, P. Rahi, R. Kumar, A. K. Sinha, and A. Gulati, Med. Chem. Res. **22**, 5129 (2013).
57. S. Hisaindee, L. Al-Kaabi, S. Ajeb, Y. Torky, R. Iratni, N. Saleh, and S. F. AbuQamar, Arab. J. Chem. **8**, 828 (2015).
58. L. Wolfgang, J. Transit. Met. Complexes **2019**, (2019).
59. M. Lingappa, N. M. Kikkeri, R. Devaraju, and S. Sreedharamurthy, Chin. J. Chem. **29**, 102 (2011).
60. I. Waziri, T. L. Yusuf, E. Akintemi, M. T. Kelani, and A. Muller, J. Mol. Struct. **1273**, 134382 (2023).
61. R. S. Bendre, R. D. Patil, P. N. Patil, H. M. Patel, and R. S. Sancheti, J. Mol. Struct. **1252**, 132152 (2022).
62. I. S. Luna, W. W. Neves, R. G. de Lima-Neto, A. P. Albuquerque, M. G. Pitta, M. J. Rêgo, R. P. Neves, M. T. Scotti, and F. J. Mendonça-Junior, J. Braz. Chem. Soc. **32**, 1017 (2021).
63. A. C. Price, K.-H. Choi, R. J. Heath, Z. Li, S. W. White, and C. O. Rock, J. Biol. Chem. **276**, 6551 (2001).

Tables

Table 1 and 4 are available in the Supplementary Files section.

Table 2
Chemical shifts (δ C in ppm) for substituted Schiff bases S_1-S_8.

Ligand	δC-6	δC-1	δC-2	δC-α	δC-1′
S_1	119.14	153.01	149.63	164.4	149.33
S_2	120.78	153.00	149.51	162.32	146.3
S_3	120.15	154.11	153.43	163.88	149.98
S_4	121.65	153.00	149.68	164.69	146.17
S_5	121.00	149.64	148.50	164.57	153.07
S_6	119.41	152.92	149.10	162.60	68.68
S_7	122.28	153.01	149.87	168.51	126.00
S_8	122.69	153.01	149.93	169.12	161.61

Table 3
Crystal data and structure refinement for S_1.

Identification code	**SHELXS**
Empirical formula	$C_{13}H_9BrClNO_2$
Formula weight	326.57
Temperature	298(2) K
Wavelength	0.71073 Å
Crystal system	Triclinic
Space group	P -1
Unit cell dimensions	a = 7.1550(6) Å, ά= 93.498(3)°.
	b = 7.7320(7) Å, β = 104.050(3)°.
	c = 12.8078(10) Å, γ = 115.471(3)°.
Volume	609.38(9) $Å^3$
Z	2
Density (calculated)	1.780 Mg/m^3
Absorption coefficient	3.583 mm^{-1}
F(000)	324
Crystal size	0.300 x 0.250 x 0.200 mm^3
Theta range for data collection	3.275 to 33.222°.
Index ranges	-11 < = h<=11, -11 < = k<=11, -19 < = l<=19
Reflections collected	41509
Independent reflections	4657 [R(int) = 0.0542]
Completeness to theta = 25.242248	99.8%
Absorption correction	Semi-empirical from equivalents
Max. And mine. Transmission	0.7465 and 0.4944
Refinement method	Full-matrix least-squares on F^2
Data/restraints/parameters	4657 / 0 / 163
Goodness-of-fit on F2	1.100
Final R indices [I > 2sigma(I)]	R1 = 0.0400, wR2 = 0.0929

Identification code	SHELXS
R indices (all data)	R1 = 0.0697, wR2 = 0.1081
Extinction coefficient	n/a
Largest diff. Peak and hole	0.765 and − 0.759 $e.^{-3}$

Table 5. Hydrogen bonds for S_1acn [Å and °].

D-H...A	d(D-H)	d(H...A)	d(D...A)	<(DHA)
C (11)-H (11)...Cl(1)#1	0.93	2.96	3.739(2)	142.4
O(1)-H(1A)...N(1)	0.82	1.84	2.572(3)	147.6
O(2)-H(2A)...O (1)#2	0.82	1.93	2.748(3)	173.2

Table 6
Antibacterial and antifungal MIC (µg/ml) of the Schiff bases.

Compounds	Gram-positive bacteria		Gram-negative bacteria		Fungi		
	S. aureus	S. pyogenes	P.aeruginosa	E. coli	C. albicans	A.niger	A.clavatus
S1	100	250	125	100	250	500	1000
S2	125	250	125	100	500	1000	> 1000
S3	100	50	100	62.5	1000	> 1000	> 1000
S4	250	500	250	250	1000	1000	> 1000
S5	100	62.5	125	250	250	500	500
S6	62.5	250	125	50	250	500	1000
S7	250	125	100	125	250	500	1000
S8	250	100	125	100	100	> 1000	> 1000
DHDPM [a]	128	-	128	128	-	-	-
DHSalen [a]	128	-	128	128	-	-	-
DHSalomphen [a]	128	-	128	256	-	-	-
Ampicillin	250	100	100	100	NT	NT	NT
Griseofulvin	NT	NT	NT	NT	500	100	100

a = Ref. [47].

Table 7
Docking score of compounds towards the Beta-ketoacyl ACP Synthase-I.

Code	Docking Score	Glide model	Glide energy
Ampicillin	-7.388	-62.038	-43.94
S_4	-6.785	-50.722	-39.286
S_3	-6.59	-44.452	-36.03
S_1	-6.557	-53.433	-39.749
S_6	-6.428	-49.516	-37.099
S_2	-6.247	-47.18	-34.936
S_5	-6.122	-52.286	-39.952
S_8	-6.05	-47.606	-37.058
S_7	-5.574	-41.72	-31.402

Schemes

Scheme 1 is available in the Supplementary Files section

Figures

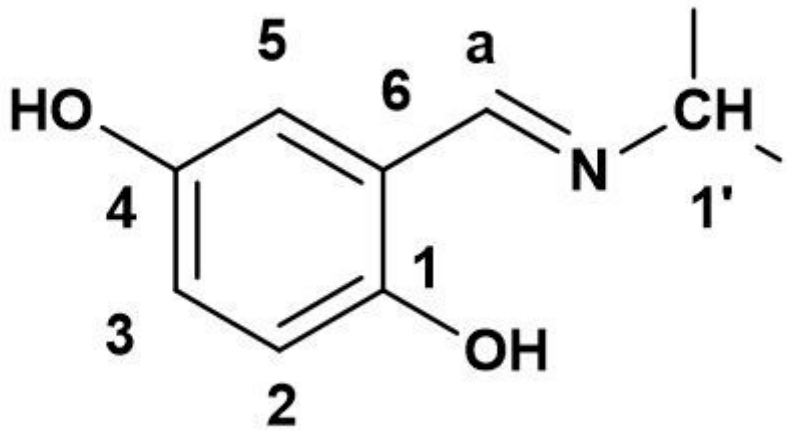

Figure 1

Legend not included with this version.

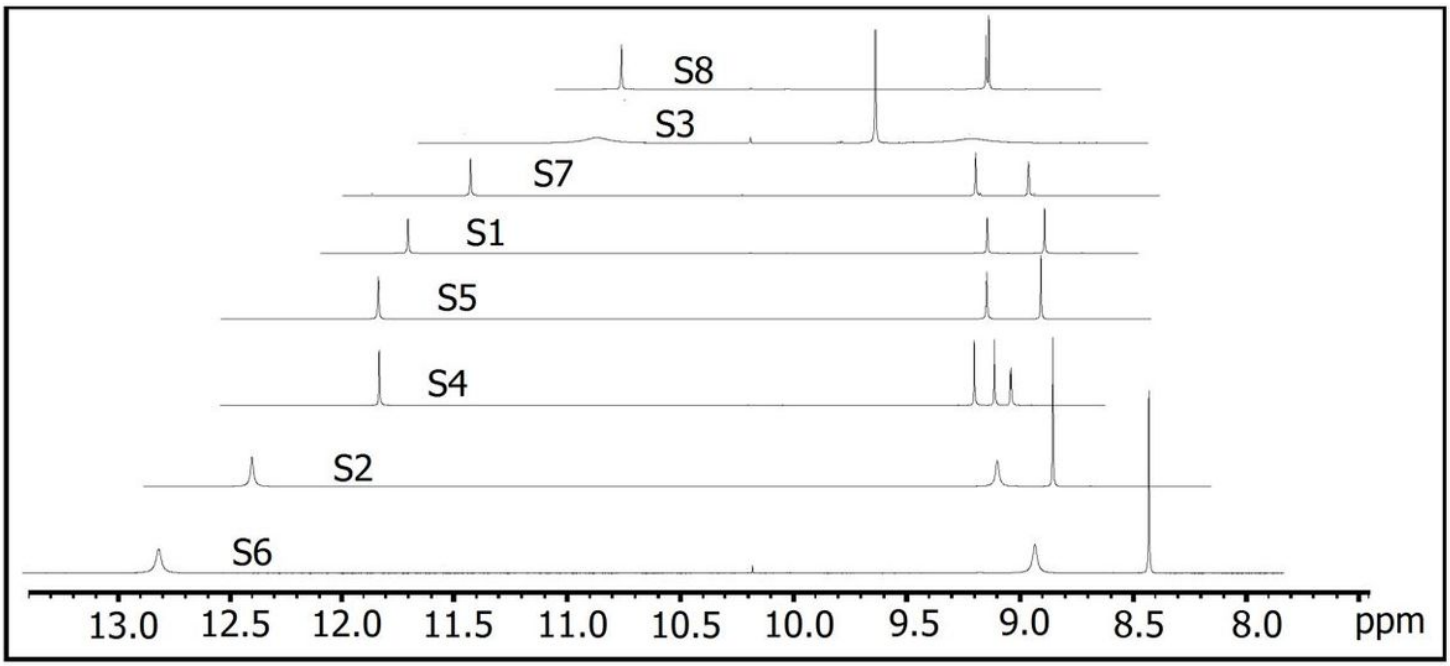

Figure 2

^{1}H-NMR Shift

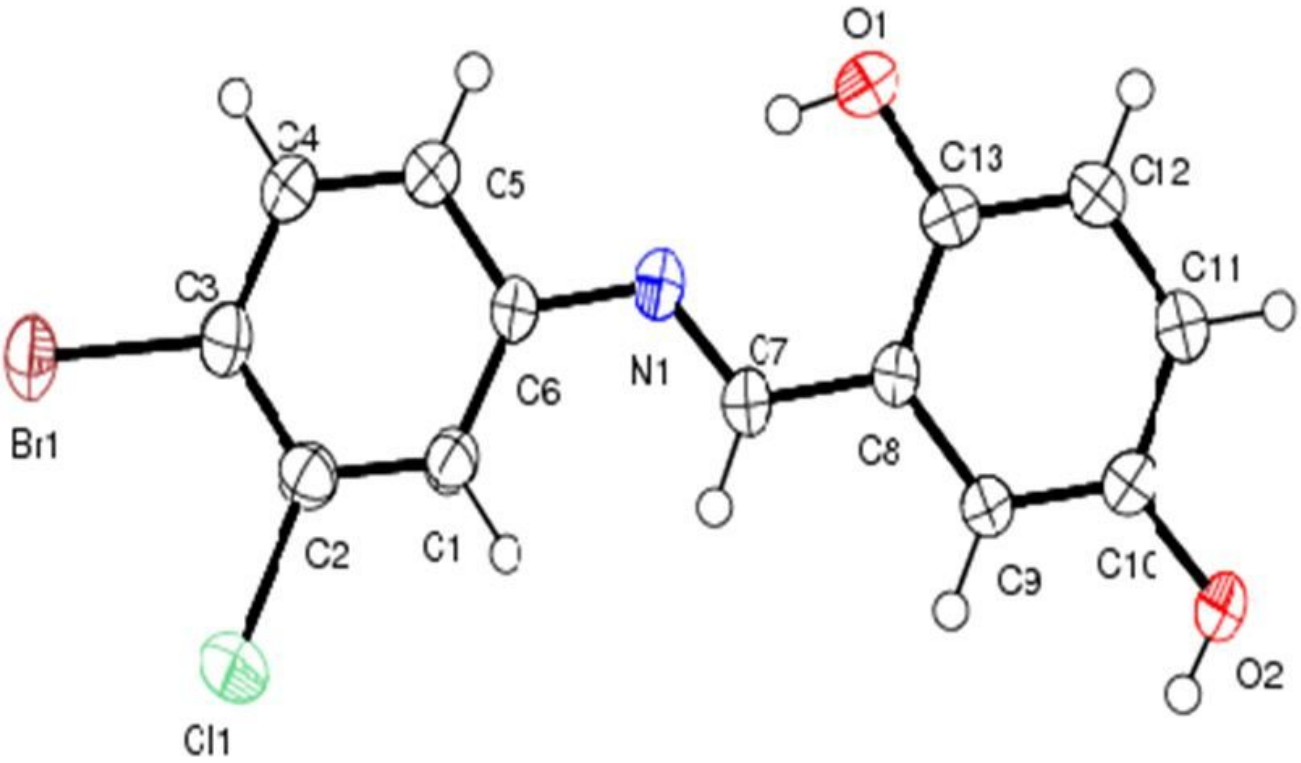

Figure 3

ORTEP of S1

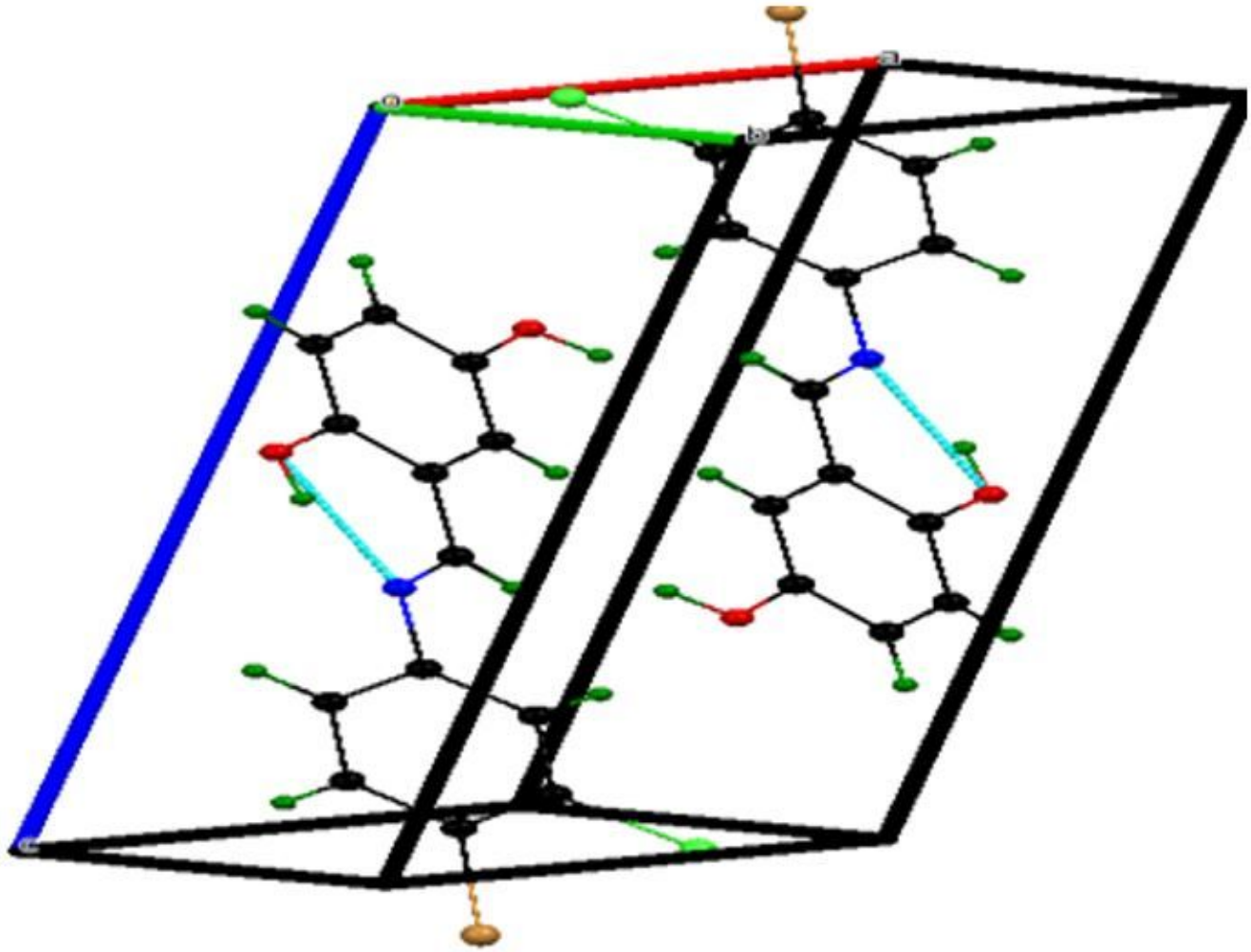

Figure 4

Pack unit cell of S_1

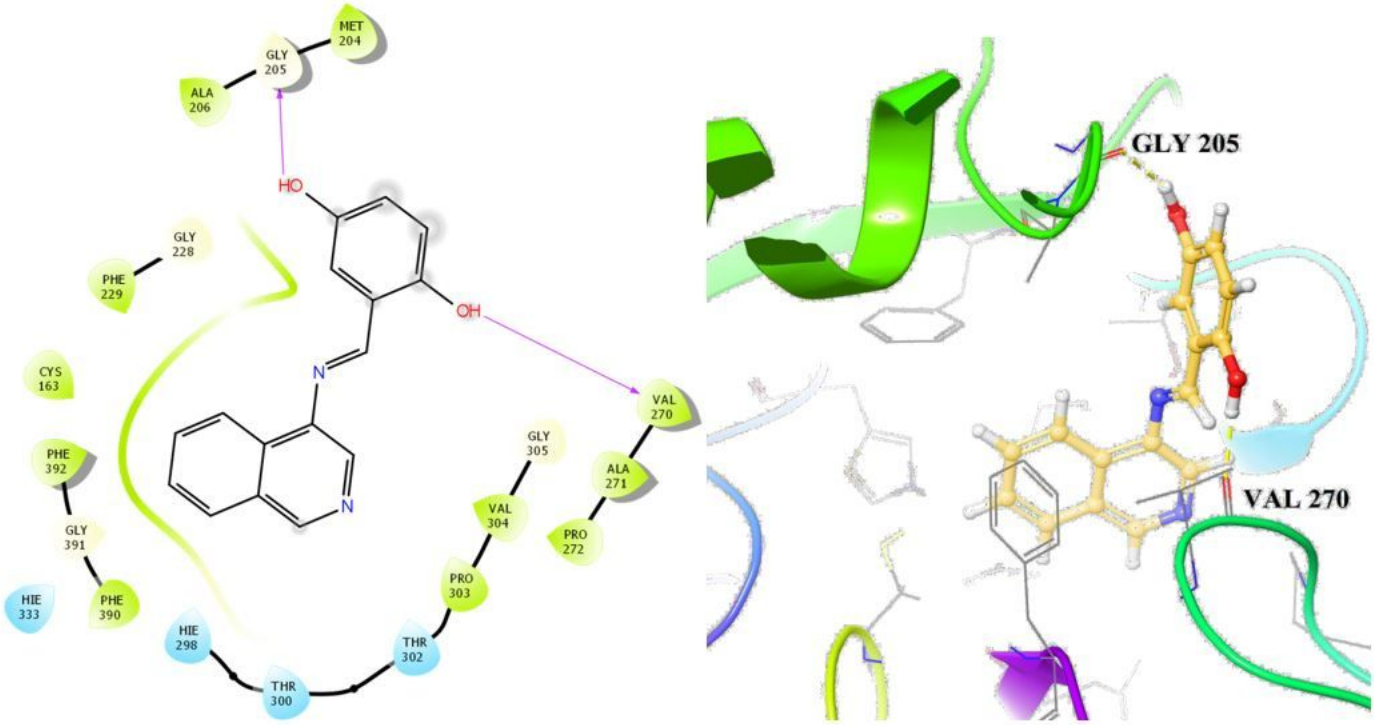

Figure 5

Interaction of S_4 with Beta-ketoacyl-[acyl Carrier Protein] Synthase I of *E.coli*

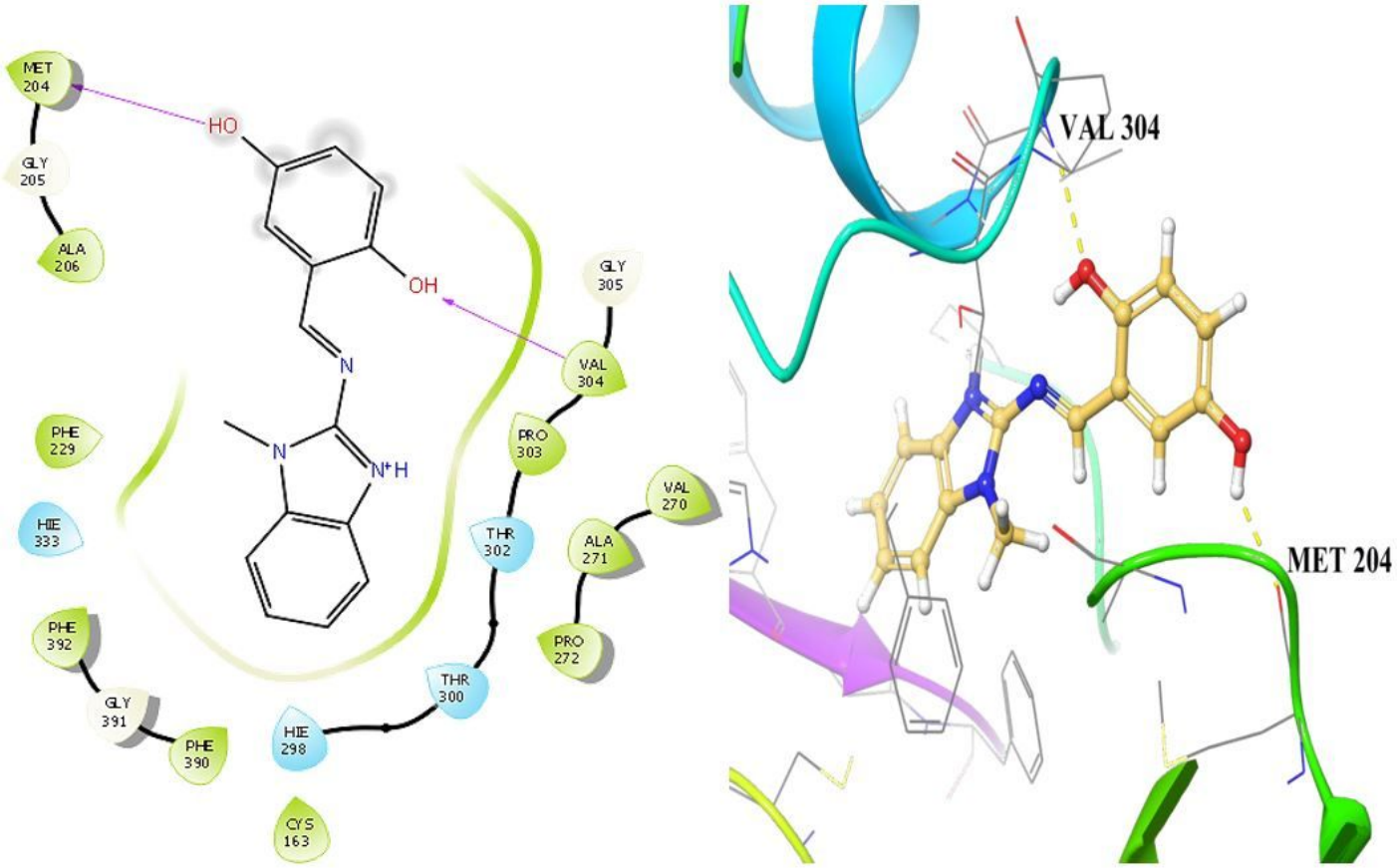

Figure 6

Interaction of S_3 with Beta-ketoacyl-[acyl Carrier Protein] Synthase I of *E.coli*

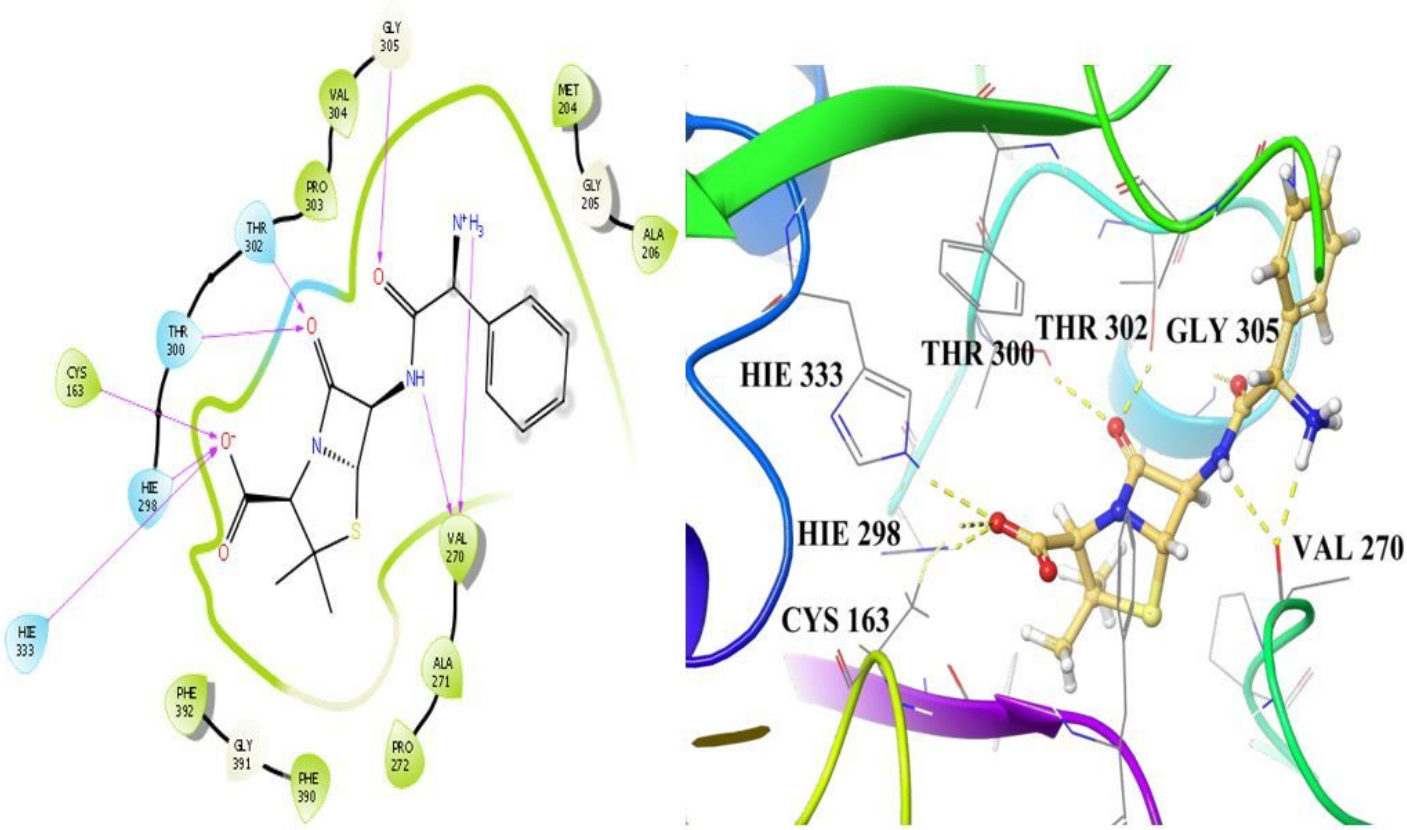

Figure 7

Interaction of Ampicillin with Beta-ketoacyl Synthase I of *E.coli*

Supplementary Files

This is a list of supplementary files associated with this preprint. Click to download.

- supplementarydataRCId1.pdf
- TablesRCI.docx
- Scheme1.jpg
- GA.jpg